

Review

Progresses of Mid-Infrared Glass Fiber for Laser Power Delivery

Xiaolin Liang ¹, Kai Jiao ¹, Xiange Wang ¹, Yuze Wang ¹, Yuyang Wang ¹, Shengchuang Bai ¹, Rongping Wang ¹, Zheming Zhao ^{2,*} and Xunsi Wang ^{1,*} 

¹ Laboratory of Infrared Material and Devices, The Research Institute of Advanced Technologies, College of Information Science and Engineering, Ningbo University, Ningbo 315211, China; liangxiaolin0622@163.com (X.L.); m15669146087@163.com (K.J.); edisonki@163.com (X.W.); 1692437099@qq.com (Y.W.); a15586539677@163.com (Y.W.); baishengchuang@nbu.edu.cn (S.B.); wangrongping@nbu.edu.cn (R.W.)

² College of Data Science, Jiaying University, Jiaying 314001, China

* Correspondence: zhaozheming@zjxu.edu.cn (Z.Z.); wangxunsi@nbu.edu.cn (X.W.)

Abstract: High-power laser delivery in infrared optical fiber has received much attention due to the urgent needs in the fields of national defense security, biomedicine, advanced manufacturing, and so on. In recent decades, there has been extensive research aimed at enhancing the capabilities of infrared laser power delivery through the purification of infrared glass or the optimization of fiber structures. This article provides an overview of common passive mid-infrared (MIR) optical fibers with numerous glasses and fiber structures, as well as their characteristics in laser power delivery. This review also highlights potential research directions and analyzes the challenges of passive mid-infrared fibers in the current applications.

Keywords: mid-infrared glass fiber; micro-structured optical fibers; laser power delivery

1. Introduction

Mid-infrared (MIR) lasers have found extensive applications in industrial processing, medical treatment, environmental monitoring, and military defense [1–3]. This requires a suitable medium to deliver the MIR light, in which MIR glass optical fiber has garnered extensive attention owing to its notable advantages, including flexible transmission and robust environmental adaptability. Currently, passive MIR glass fibers can be classified into step-index and micro-structured fibers (MOF) based on their waveguide structures. Generally, the characters of step-index fibers are directly derived from their glass host. Therefore, these fibers can be classified into categories such as heavy metal oxide glass fiber [4], fluoride glass fibers [5], and chalcogenide (CHG) glass fibers et al. [6]. Compared with silica-based fibers, there is significant room for improvement in the performance of MIR optical fibers in terms of losses and laser delivery capabilities. Presently, research in MIR fibers primarily focuses on improving fiber manufacturing techniques for low loss and expanding the range of glass hosts for high laser-induced damage threshold (LIDT). Traditional large-mode area fibers can deliver a relatively larger power due to the suppression of the nonlinear effects, but they fall short of achieving the high-quality transmission of single-mode characteristics. The emergence of MOF provides a solution to this situation. This unique fiber structure not only enables continuous single-mode transmission but also facilitates larger mode area. However, they are currently hindered by exceeding fiber losses and low flexibility.

In recent decades, to meet diverse power delivery requirements, researchers have explored numerous glass hosts and fiber structures for MIR energy transmission. This paper summarizes recent advancements in passive MIR glass fiber for laser transmission, and discusses some primary challenges encountered in its development.



Citation: Liang, X.; Jiao, K.; Wang, X.; Wang, Y.; Wang, Y.; Bai, S.; Wang, R.; Zhao, Z.; Wang, X. Progresses of Mid-Infrared Glass Fiber for Laser Power Delivery. *Photonics* **2024**, *11*, 19. <https://doi.org/10.3390/photonics11010019>

Received: 30 November 2023

Revised: 24 December 2023

Accepted: 25 December 2023

Published: 26 December 2023



Copyright: © 2023 by the authors. Licensee MDPI, Basel, Switzerland. This article is an open access article distributed under the terms and conditions of the Creative Commons Attribution (CC BY) license (<https://creativecommons.org/licenses/by/4.0/>).

2. Step Refractive Index Fibers

2.1. Heavy Metal Oxide Glass Fiber

Heavy metal oxide glasses are composed of various systems, such as bismuth oxide, tellurite, and germanate glasses. These glasses can offer several advantages over traditional oxide glasses, including lower phonon energy and higher LIDT [7]. Among these, the tellurite glass system has received particular attention due to its broad infrared transmission spectrum. Researchers have incorporated a specific amount of fluoride into tellurite glass, and fluorotellurite glass exhibits higher LIDT and better thermal stability compared to traditional tellurite glass. However, heavy metal oxide glasses generally have relatively higher losses (1.7 dB/m@1980 nm) [4] owing to limitations in glass purification processes and fiber fabrication. Specifically, at 4000 nm and 3000 nm, the LIDT reached 1.08 J/cm² and 0.852 J/cm², respectively [8]. The results are valuable for the utilization of fluorotellurite glasses in high-powered fiber laser applications. Figure 1 illustrates the change in TBY60 glass with the number of pulses and energy threshold, and the inset is the comparison of the damage under 3 μm and 4 μm irradiation at the same laser power.

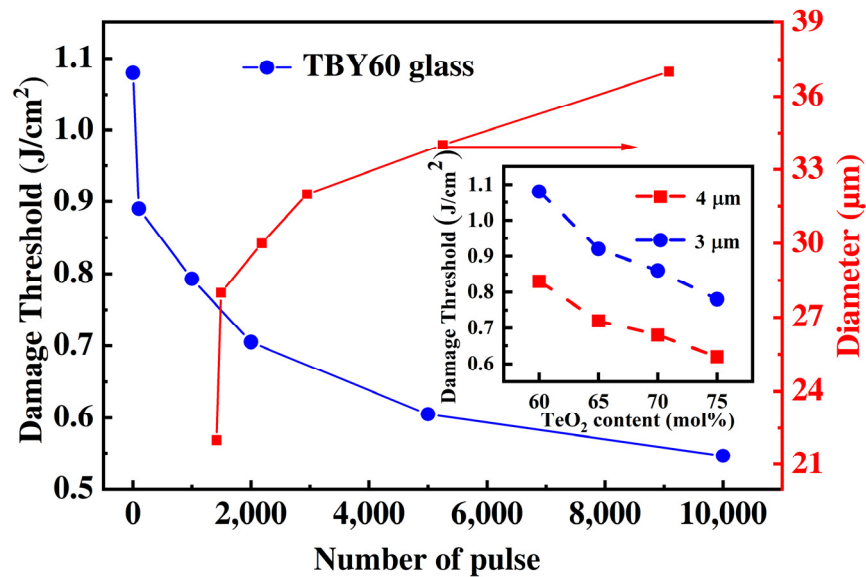


Figure 1. Changes in the number of pulses reflect the trend of LIDT and the diameter of damaged craters in TBY60 glass. The inset illustrates LIDT under 3 μm and 4 μm irradiation at the same laser power.

2.2. Heavy Metal Fluoride Glass Fiber

Fluoride glass refers to non-crystalline glass materials composed of fluorine as the anion. Fluoride glasses offer several advantages, including high transmittance, high damage threshold, and excellent rare-earth ion solubility [9]. The development of fluoride glass dates back to 1975, when M. Poulain [10] created ZrF₄-based fluoride glass in France. Subsequently, AlF₃-based glass fibers were developed. In particular, the fiber loss of ZBLAN is as low as 0.025 dB/km, and several related products have been successfully introduced into commercial markets.

In 1989, Whitehurst [11] conducted a laser damage experiment on ZBLAN glass fibers at 2.94 μm. The highest power delivery was 3.5 W, with an energy density of up to 1.0 kJ/cm² (peak power density reaching 10.2 MW/cm²). Subsequently, Wuthrich [12] continued his research on the optical damage thresholds of single-mode and multi-mode fluoride glass fibers at 2.94 μm. The results showed that the optical fibers could withstand a maximum power density of only 0.08 MW/cm². Figure 2 shows the findings from their research. A notable difference in the damage threshold of ZBLAN glass fibers was observed, primarily attributed to the deliquescent nature of ZBLAN glass [13,14]. The lower resistance to deliquescence significantly impacts the operational lifetime of ZBLAN glass fibers.

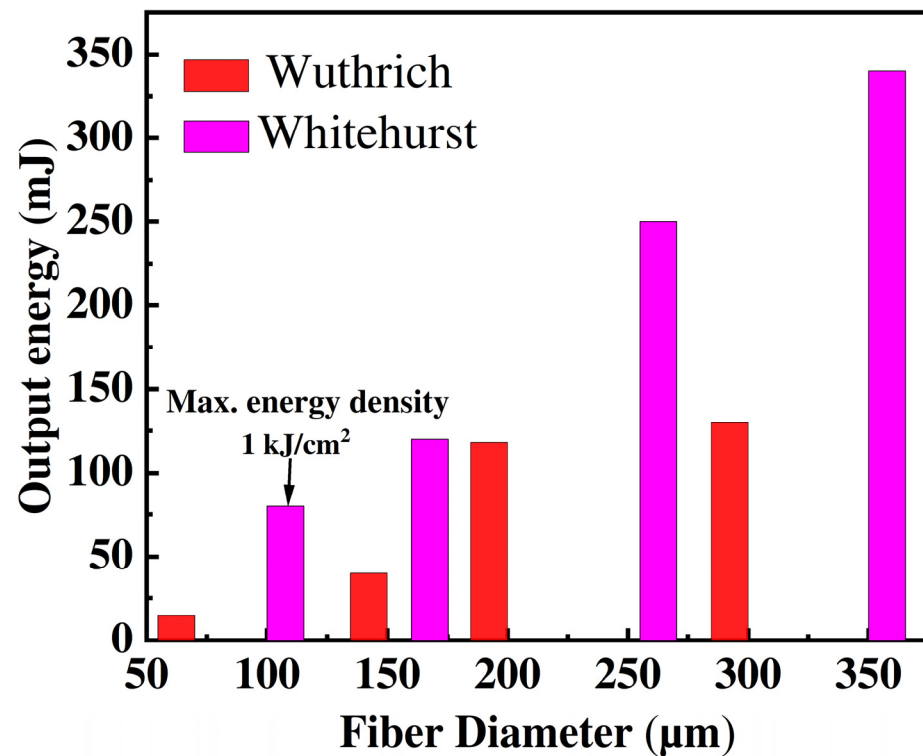


Figure 2. Illustrates the maximum energy transmission threshold of Er: YAG lasers in ZBLAN optical fibers with varying core diameters, as determined by Wuthrich and Whitehurst.

Subsequently, researchers explored non-ZrF₄-based fluoride glass optical fibers, such as the AlF₃ glass fiber. Compared to ZrF₄-based glasses, AlF₃-based glasses exhibit a higher glass transition temperature (375 °C) and enhanced chemical stability. In 1994, Itoh et al. [15] reported an AZBCY (AlF₃-ZrF₄-BaF₂-CaF₂-YF₂) fiber with a loss below 0.1 dB/m at 2.94 μm. This fiber could deliver a maximum output power of 8.7 W using an Er: YAG laser, and the power density reached as high as 80 kW/mm². In 2018, Aydin [16] reported a study on the stability of AZBCY optical fibers in high-power laser systems. In this experiment, the replacement of ZBLAN glass with AlF₃-based glass extended the continuous working time from 10 min to 7 h at a fixed 3 μm lasers power of 20 W, confirming the material advantages of AlF₃-based glass under high-power operating conditions. Consequently, AlF₃-based glass fiber is a highly promising medium for delivering a 3–5 μm wavelength laser. In summary, compared to the commercial ZrF₄-based glass, AlF₃-based glass demonstrates superior resistance to laser-induced damage. This makes it exceedingly beneficial for transmitting 3 μm wavelength lasers.

2.3. Chalcogenide Glass Fiber

Chalcogenide glasses are composed of chalcogen elements S, Se, and Te, along with the addition of other elements such as Ge, As, and Sb, resulting in the formation of stable glasses. CHG glass materials possess exceptionally low phonon energy (300–450 cm⁻¹), enabling low-loss transmission in the range of 2–12 μm [17]. Furthermore, in comparison to the fluoride glasses, the chalcogenide (ChG) glasses possess a wider glass forming region, along with much longer infrared cut-off edge and significantly higher thermal and chemical stability [18]. CHG glass fibers have been widely used in infrared laser transmission, particularly in wavelengths such as 3–5 μm and 10.6 μm.

2.3.1. Progress in Laser Delivery below 5 μm Wavelength

The initial research on CHG glasses started with relatively simple compositions of the As-S system. The inaugural CHG glass fiber emerged in 1965 through Optics Technology

in the United States [19]. Step-index structured fibers are the earliest form of CHG glass fibers. This section will focus on the research developments of step-index CHG glass fibers in the 2–5 μm laser delivery range.

In 1996, the US Naval Research Laboratory conducted an in-depth investigation into the transmission properties of As-S-Se fibers for infrared pulsed lasers [20]. No damage was observed at the fiber’s end face when transmitting low-repetition-rate (1–10 Hz) pulsed lasers with an average power below 100 mW. Subsequently, the fiber remained undamaged even after several minutes of exposure when transmitting a high-repetition-rate (10^4 Hz) pulsed laser with an average power below 1 W. A 1 m long As-S-Se fiber could withstand maximum peak power densities of 49.8 MW/cm² for 2 μm HO³⁺: YLF and 9 MW/cm² for 3.3 μm KTP OPO pulsed laser delivery. In 1998, Sanghera et al. [21] reported the transmission of an 18 mJ pulse Medical Free Electron Laser (MFEL) operating at 2.94 μm using a multimode As-S fiber. Additionally, they observed that the fiber end-face could withstand a 2–5 μm pulsed laser with a peak power of 16.9 kW for 1.5×10^7 pulses, corresponding to a laser power density of 1.07 GW/cm² [22].

In 2007, Papagiakoumou et al. [23] prepared two types of multimode fibers with a large core diameter of 1000 μm for Er³⁺: YAG lasers transmitting at a wavelength of 2.94 μm. The first is based on As-Se-Te, with a loss of 0.7 dB/m, and the other is based on As-S, with a loss of 1.5 dB/m. The results indicate that, for pulse durations of 80 μs, the maximum input energy of the pulsed laser was 4.6 mJ, corresponding to a power density of 81.5 kW/cm². For pulse durations of 190 ns, the maximum input energy of the pulsed laser was 2.3 mJ, corresponding to a power density of 28.2 MW/cm². In 2022, Qi et al. [24] demonstrated a power transmission of 100 W in multi-mode As-S fibers using a high-power 2 μm erbium-doped silicon fiber laser source. With effective cooling, the 200 μm core diameter As-S multimode fibers resisted an incident laser power of 120 W, transmitted 63 W, and handled an incident power density of up to 472 kW/cm². The results are shown in Figure 3a.

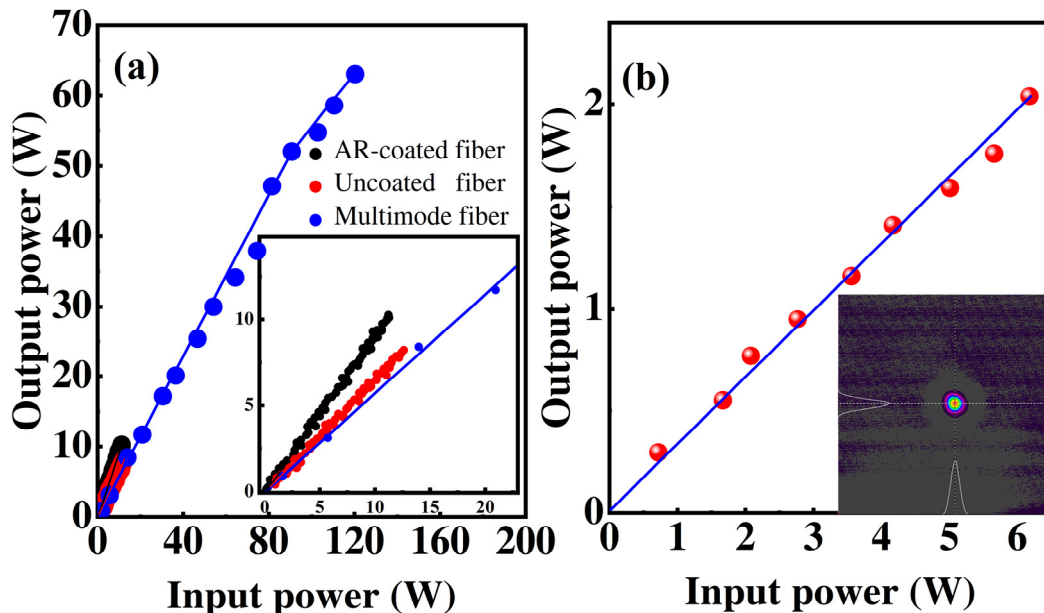


Figure 3. (a) Power transfer in As-S fiber at 2 μm wavelengths; (b) Output power transmission versus input power using a 3.8–4.7 μm laser source through a 0.5 m long fiber.

Currently, CHG glass fibers have achieved a power delivery of over 50 W in the 2–5 μm band. However, in critical fields like medical surgery and military defense, achieving a high-quality output beam is still a primary task for laser delivery. In 2015, Chenard et al. [25] reported a single-mode As-S fiber, in which no laser-induced damage is visible under the pumping of a CW laser power of 3.5 W at 2 μm. In 2018, Sincore et al. [26] applied an

antireflection (AR) coating on the surface of the As-S fiber and achieved a transmission record of $90.6 \pm 0.3\%$ at $2 \mu\text{m}$. Although the AR-coating significantly benefits the laser delivery, cracking may occur in the fiber with prolonged exposure to a high power laser. Specifically, damage features were observed in the polymer coating after coupling 1.3 W power at the end face of the fiber at $2.5 \mu\text{m}$, and the fiber was damaged at a coupling power of 1.1 W (the facet ignited) at $4.1 \mu\text{m}$. In 2022, Liang et al. [27] fabricated a Ge-As-S single-mode fiber by a double peeling-off extrusion method for the first time. The lowest loss of this Ge-As-S single-mode fiber is 0.41 dB/m . In transmission experiments, the fiber withstood long-pulse lasers (wavelength $3.8\text{--}4.7 \mu\text{m}$) at 6.2 W , with a high optical power density of 1.97 MW/cm^2 and an approximate transmission efficiency of 30% , as depicted in Figure 3b.

2.3.2. Progress in Laser Delivery above $5 \mu\text{m}$ Wavelength

The CO laser of $5 \mu\text{m}$ and the CO_2 laser of $10.6 \mu\text{m}$ have been utilized in laser medical surgery, industry cutting, and many other domains. Current, the loss of CHG fibers in the $5\text{--}12 \mu\text{m}$ region has been reduced to below 1 dB/m . Researchers are exploring the application of CHG fibers in the transmission of CO and CO_2 lasers.

(1) Transmission of CO laser in CHG fiber

In 1984, Dianov et al. [28] reported a 1.5 m long Ge-As-Se CHG fiber for continuous CO laser transmission at $5.3 \mu\text{m}$. They achieved a power output of $6\text{--}7 \text{ W}$, and the power density of the fiber was up to about 2 kW/cm^2 . In the same year, Hattori et al. [29] conducted CO laser transmission experiments at $5.3 \mu\text{m}$ using As_2S_3 bare fibers with core diameters of $500 \mu\text{m}$ and $1000 \mu\text{m}$, and lengths of 130 cm and 420 cm , respectively. These fibers exhibited a loss of 0.3 dB/m at $5.3 \mu\text{m}$, with maximum output powers of 19.7 W and 39 W , respectively. The maximum laser damage threshold at the fiber reached 10 kW/cm^2 . Following this, Arai et al. [30] performed laser experiments in the same wavelength range using As_2S_3 fibers with a $200 \mu\text{m}$ core diameter, achieving a continuous laser output of 4 W with a laser power density of 12.8 kW/cm^2 .

In 1985, Watanabe [31] etc. discovered that the As_2S_3 fiber exhibited a minimal transmission loss of 0.3 dB/m around the $5.3 \mu\text{m}$ wavelength. Under the conditions of 100 cm length and $1000 \mu\text{m}$ core diameter, the As_2S_3 multimode fiber can support a maximum output power of 59 W and a laser power density of approximately 5 kW/cm^2 at the fiber output end. In 1986, Sato [32] conducted transmission experiments of CO lasers at $5 \mu\text{m}$ using the As_2S_3 fiber with a polytetrafluoroethylene (PTFE) coating. When the incident laser power was 100 W , the laser power at the fiber output end was 62 W with a laser power density of 16 kW/cm^2 . In 1988, Arai et al. reported [33] an As_2S_3 optical fiber with FEP cladding and core diameter of $400 \mu\text{m}$, and the fiber can transmit 15.3 W (with a power density of approximately 12.2 kW/cm^2). In 1993, Sato et al. further improved the fiber with an increased core diameter of $1000 \mu\text{m}$, making it capable of transmitting a continuous laser with a power of 226 W [34] (approximately 28.8 kW/cm^2 power density), which is also the highest record reported so far. Additionally, this team also conducted laser tests on Ge-As-S fibers in this wavelength range, achieving a maximum output of 180 W with a power density of 23 kW/cm^2 . Both types of fibers exhibit the capability to transmit CO laser power at a level of several hundred watts, fulfilling the requirements for laser surgery and laser processing. In 1996, the Naval Research Laboratory [20] reported a low-loss As-S fiber ($0.75 \text{ dB/m@}4.8 \mu\text{m}$) with a core diameter of $200 \mu\text{m}$ and a length of 1 m for CO laser transmission experiments. This fiber can withstand a laser power of 6.2 W (power density of approximately 126 kW/cm^2) and achieves an efficiency greater than 60% . Other work [35] demonstrated that a low-loss, small-core ($<150 \mu\text{m}$) CHG fiber could withstand a CO laser power density of up to 124 kW/cm^2 . Figure 4 summarizes the current transmission performance of As-S fibers for mid-IR CO lasers.

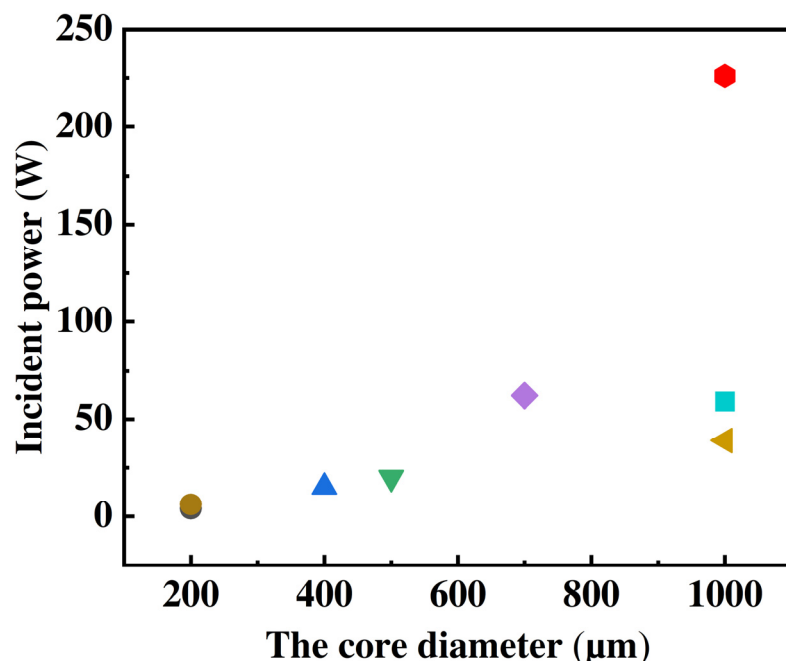


Figure 4. CO laser power transmitted by As-S fiber with different diameters.

(2) Transmission of CO₂ laser in CHG fiber

Typical CHG fibers capable of transmitting wavelengths above 10 μm include Se- and Te-based glass, with Te-based glass demonstrating the lowest loss at 10.6 μm . In the realm of CO₂ laser transmission, Nishii [36] fabricated CHG glass fibers with core and cladding glass compositions of Ge-Se-Te and Ge-As-Se-Te in 1989. The core and cladding diameters were 340 μm and 440 μm , respectively. These fibers exhibited a loss of 1.8 dB/m at a wavelength of 10.6 μm . The maximum delivery power reached 1.8 W for a 1.5 m long fiber. Following this, Nishii [37] employed a dual crucible technique to produce Ge-Se-Te and Ge-As-Se CHG glass fibers, exhibiting losses of 1.8 dB/m and 5.2 dB/m at 10.6 μm , respectively. With core and cladding diameters of 450 μm and 560 μm , respectively, the 1 m-long fibers yielded maximum CO₂ laser outputs of 4.6 W and 2.2 W, corresponding to power densities of 2.9 kW/cm² and 1.4 kW/cm². In 1991, Inagawa et al. [38] reported a Se-Te-I multimode fiber with a loss of 0.9 dB/m at 10.6 μm . With an input power of 2.85 W from the CO₂ laser, an output power of 0.82 W can be obtained through the unprotected fiber.

In 1996, Busse et al. [20] reported the use of Ge-As-Se-Te multimode optical fibers for CO₂ laser transmission. The fiber core and cladding diameters were 162 μm and 270 μm , respectively. The experiment recorded the maximum input and output powers of 1.73 W and 0.6 W, achieving a transmission efficiency of 34.7%, with a maximum input power density of 27 kW/cm². Su et al. [39] fabricated a Ge-As-Se-Te multimode optical fiber with a loss of 5 dB/m at 10.6 μm . Despite having a higher loss than Se-Te-I fiber, this type of fiber demonstrates higher chemical stability and damage thresholds. During the coupling of CO₂ lasers into CHG fibers, and to prevent laser overheating, the laser exposure time was limited to 60 seconds, and the fibers were subjected to air cooling. The results indicate that a maximum input power of 6.16 W and an output power of 1.37 W could be obtained in the fiber without any damage. The respective laser power densities at the input and output ends of the fiber were 4.9 kW/cm² and 1.09 kW/cm².

The laser transmission performance of different step-index fibers is presented in Table 1. Significant progress has been achieved in CHG step-index fibers for MIR laser power delivery. Presently, multimode fibers can deliver the laser power of over a hundred watts, while single-mode fibers can effectively fulfill laser transmission up to 10 W. These fibers have been experimentally validated in fields such as laser surgery and laser processing. Israel and Russia have successively initiated research on fiber-based CO₂ laser scalpels,

with related products already available in the market. However, although selenium and telluride glass fibers can be used for CO₂ laser transmission at 10.6 μm, their refractive index temperature coefficients ($dn/dT = 3 \times 10^{-5}$ – $14 \times 10^{-5} \text{ K}^{-1}$) are notably higher than that of As-S ($1 \times 10^{-5} \text{ K}^{-1}$). This higher coefficient often leads to the occurrence of self-focusing effects, resulting in a relatively lower LIDT for fiber.

Table 1. Laser transmission performances of different chalcogenide fibers.

Laser Wavelength (μm)	Fiber Material	D * (μm)	Laser Transmission (W)	Year	References
2	As-S	9	2.1	2015	[25]
		200	63	2022	[24]
2.05	As-S	12	10.3	2018	[26]
2.52			1.3		
4.1			0.5		
3.8–4.7	Ge-As-S	20	2.1	2022	[27]
5	As-S	1000	39	1984	[29]
	As-S		226	1993	[34]
	Ge-As-S		180	1993	[34]
10.6	Ge-As-Se	560	2.2	1990	[37]
	Se-Te-I	400	0.82	1991	[38]
	Ge-As-Se-Te	400	1.37	2019	[39]

* D is the core diameter.

3. Micro-Structured Fibers

Although traditional large-mode area fibers can deliver relatively greater power by suppressing nonlinear effects, they fall short of achieving the high-quality transmission associated with single-mode characteristics. The emergence of the Photonic Crystal Fiber (PCF) has presented a new approach to address this challenge. The infinite single-mode and large-mode field characteristics of the PCF are of great interest in laser energy transfer research. Hence, the design and fabrication of a low-loss, single-mode, large-mode area photonic crystal fiber (LMA-PCF) have become a focal point.

PCF can be classified into refractive index-guided and photonic bandgap fibers based on different light-guiding mechanisms. In 1996, Knight et al. [40–42] developed the first PCF using a light-guiding mechanism based on total internal reflection. The silica fiber has good mechanical and chemical stability, but the fiber loss is over 60 dB/m after exceeding a 3 μm wavelength. The hollow-core PCF (HC-PCF) presents an appealing alternative, directing the majority of light in air or a controlled gas composition, minimizing loss contributions from material absorption. Guiding light in a hollow core also provides a higher damage threshold and additional functionalities. For example, in 2012, Ulrich et al. [43] demonstrated the ability to deliver, for the first time, high energy microsecond pulsed Er: YAG laser light at a wavelength of 2.94 μm through a silica HC-PCF. The average loss in the wavelength range from 2.9 μm to 3.15 μm was ~1.2 dB/m and the loss at the wavelength of the Er: YAG laser was 1.1 dB/m. The output power was measured for 5 min (4425 pulses) at 180 mW with no observable damage to the launch facet. Currently, the PCF is extensively used in nonlinear optics, optical communication, and photonic devices.

Soft glass materials (e.g., sulfide glass, fluoride glass) exhibit lower absorption losses within the mid-infrared band, making them extensively employed in this spectral range. A PCF based on Ga-La-S CHG glass with a high nonlinear coefficient and wide transmission range was fabricated in 2000 [44]. In 2007, Troles et al. [45] fabricated CHG glass LMA-PCF, where a mode field area of 1000 μm² was achieved. Theoretically, the mode field area of CHG LMA-PCF can be increased to tens of thousands while maintaining single-mode

transmission. In the advancement of LMA-PCF, scientists have introduced an all-solid design, and this design prevents defects caused by pore deformation during fiber drawing, ensuring minimal influence from environmental factors on fiber transmission. In 2019, Ren et al. [46] fabricated an all-solid LMA-PCF with a mode field area of $5200 \mu\text{m}^2$ and a fiber loss of 5.2 dB/m at a wavelength of $4 \mu\text{m}$. In 2020, Feng et al. [47] presented a few-mode LMA-PCF for high-power mid-infrared laser delivery, with a fiber loss of 7.8 dB/m at a wavelength of $2 \mu\text{m}$. Numerical simulations indicated a mode field area of $10,500 \mu\text{m}^2$. The fiber end-face was damaged at an incident power of 11.8 W. For continuous-wave laser in $2 \mu\text{m}$, the maximum allowable incident laser power density is estimated to be $150 \text{ kW}/\text{cm}^2$.

Looking at the overall scenario, the current minimal loss of CHG glass LMA-PCF stands below 10 dB/m, and the deviation from theoretical losses is large. This discrepancy primarily arises due to the composite nature of total losses in LMA-PCF, which includes material absorption, defect-induced losses, and bending losses. Indeed, air or even a vacuum is considered as optimal mediums for light wave transmission. In such environments, light waves propagate with minimal distortion and at the fastest speed in lossless, non-dispersive conditions. In 2002, Temelkuran et al. [48] reported Hollow-core Bragg fibers (HC-BFs) composed of $\text{As}_{40}\text{Se}_{60}$ glass and a PES cladding. The fiber demonstrated a wavelength transmission range from 0.75 to $10.6 \mu\text{m}$, with a fiber loss of less than 1 dB/m at $10.6 \mu\text{m}$. Additionally, achieving a maximum laser delivery power density of about $300 \text{ W}/\text{cm}^2$ by a CO_2 laser. This verifies the feasibility of achieving low-loss transmission through structural design. However, HC-BFs are highly sensitive to manufacturing tolerances, so their theoretical transmission loss tends to be from two to three orders of magnitude higher than that of Hollow-core Anti-resonant Fibers (HC-ARFs) [49].

The light-guiding mechanism of HC-ARF, also known as negative curvature fiber, can be traced back to the anti-resonant planar waveguide theory proposed by Duguay et al. in 1986 [50]. In 2002, Benabid et al. reported a specific type of hollow-core fiber with a cladding structure referred to as the Kagome structure [51]. The Kagome structure fiber deviates from the optical propagation theory of photonic bandgap fibers structurally, but optical can propagate within the fiber core. This hollow-core fiber was named HC-ARF. In 2011, Pryamikov et al. [52] demonstrated the possibility of guiding light in the mid-infrared spectral range ($>3.5 \mu\text{m}$) using a silica HC-ARF, although the material loss of silica glass is notably high. In 2019, Yu et al. [53] prepared an ultra-low-loss HC-ARF by adjusting the parameters, achieving a record of mid-infrared silica-based hollow fiber with a loss of 18 dB/km at a wavelength of $3.1 \mu\text{m}$. This significantly reduces the absorption limit of silica materials.

Negative curvature fibers combine wide-band transmission with low theoretical losses and high manufacturing tolerances. This is particularly crucial for multi-component glasses like CHG glasses. In 2016, Gattass et al. [54] report the fabrication As_2S_3 HC-ARF using an extrusion method. At a wavelength of $10 \mu\text{m}$, the fiber exhibited minimal loss at 2.1 dB/m, marking a significant reduction in losses by 2–3 orders of magnitude compared to As_2S_3 step-index fibers at the same wavelength. This indicates the practical applicability of the fiber for laser power delivery. In 2023, Zhang et al. [55] developed a CHG glass HC-ARF comprising seven contacting capillaries. The research, through theoretical modeling and experimental validation, emphasized the fiber's capability to suppress higher-order modes and identified several low-loss transmission windows within the mid-infrared spectrum. The measured fiber loss achieved an impressive low of 1.29 dB/m at $4.79 \mu\text{m}$, laying a solid foundation for the fabrication and application of various chalcogenide glass hollow-core anti-resonant fibers (HC-ARFs). Table 2 summarizes the properties of several representative CHG MOFs.

Table 2. Properties of several representative CHG MOFs.

Year	Fiber Material	Structure	Loss (dB/m)	Power Density (kW/cm ²)	References
2010	Te-As-Se	HC-PCF	6@9.3 μm	-	[56]
2020	Ge-As-Se	PCF	8@2 μm	150 (2 μm)	[47]
2002	As-Se	HC-BF	1@10.6 μm	0.3 (10.6 μm)	[48]
2011	Te-As-Se	ARF	13@10.6 μm	-	[57]
2016	As-S	ARF	2.1@10 μm	-	[54]
2023	As-S	HC-ARF	1.3@4.8 μm	-	[55]

In addition, there has been significant progress in the research of other soft glass infrared HC-ARFs. In 2019, Tong et al. [58] reported on the HC-ARF consisting of six non-contact capillaries using telluride-based materials. They conducted initial simulations and experimental studies on the transmission and polarization characteristics. In 2020, Perevoschikov et al. [59] presented the first borosilicate soft glass-based hollow-core fiber. The minimal losses within the near-infrared (0.8–1 μm) and mid-infrared (2–4 μm) transmission windows were measured as 0.6 dB/cm and 1 dB/cm, respectively. This development offers a new material choice for the preparation of MIR hollow-core fibers.

In summary, the fabrication of low-loss, durable, and bend-insensitive fibers at wavelengths extending to longer wavelengths and into the mid-infrared (mid-IR) is desirable for applications including high-power laser beam delivery, gas sensing, gas lasers, and surgery. Toward this goal, several materials have been explored, starting with silica glass, chalcogenide glasses, followed by fluoride and tellurite fibers. However, these glass fibers are limited by the purification of infrared glass or the optimization of the fiber structure, leading to few reports on laser power delivery.

4. Challenges Faced by MIR Fiber

Fiber optics serve as a medium for delivering mid-infrared lasers, enabling optical systems to achieve greater compactness and portability. Consequently, research on mid-infrared optical fibers marks a significant breakthrough in advancing the mid-infrared laser field. Despite substantial progress in the preparation and application research of infrared energy-transmitting glass fibers, several crucial scientific questions still require in-depth exploration:

(1) Despite the excellent optical performances of the traditional ChG glass fiber, its low laser damage threshold, arising from the weak chemical bonds constructing the glass network structure, hinders ChG glass fiber from resisting high power. Therefore, one of the pivotal future research directions involves the development of novel purification and preparation methodologies for CHG glasses with a Ge base.

(2) Fluoride glass fibers are considered the most promising non-silica-based fibers for ultra-low-loss fiber optics for long-distance communication. The theoretical lowest losses in the 1–5 μm infrared band are within the range from 10⁻² to 10⁻³ dB/m. However, the developed fibers have significant discrepancies from these theoretical predictions. The primary technical challenges include the purification of glass materials and the fiber manufacturing process. These aspects represent the focal areas for the future development of fluoride glass infrared transmission fibers. Compared to fluoride glass fibers, heavy metal oxide infrared glasses are more suitable for manufacturing practical, low-loss fibers used to transmit high-power mid-infrared lasers below 3 μm. However, the non-intrinsic loss of heavy metal oxide glass fiber remains high due to the presence of impurities like hydroxyl groups and metal particles in the glass. Therefore, reducing the non-intrinsic

loss of optical fibers is critical to enhancing the heavy metal oxide glass fibers for laser transmission efficiency.

(3) For now, the MIR MOFs have provided infinite possibilities for the mid-infrared energy transmission fiber field. The unique fiber structure not only enables continuous single-mode transmission but also facilitates larger mode area. For example, addressing issues such as coupling between MOFs and light sources. Additionally, despite the continual reduction in bending losses of MIR MOFs through structural optimizations, there still remains a noticeable gap compared to step-index fibers. Bridging this difference will be a crucial focus in the future research of MIR MOFs fields.

5. Conclusions

MIR energy transmission fibers have significant application value in national defense security, biomedicine, and other fields. Soft glass materials like CHG glass and tellurite glass demonstrate exceptional performance, expanding the range of materials available for the preparation of MIR energy-transmitting optical fibers. Presently, MIR energy transmission fibers remain behind silica-based fibers in terms of optical transmission performance and thermal stability. However, continuous advancements in MIR fiber fabrication techniques are anticipated to substantially enhance the performance of MIR glass fibers. We can expect that, in the near future, with the continuous improvement in various technologies, the MIR energy transmission fibers will move from experimental research to practical applications which will play a unique role in scientific research and production.

Author Contributions: Conceptualization, X.W.; methodology, S.B., Z.Z. and R.W.; investigation, K.J., X.W., Y.W. (Yuze Wang) and Y.W. (Yuyang Wang); writing—original draft preparation, X.L.; writing—review and editing, S.B.; visualization, X.L.; supervision, X.W.; project administration, X.W.; funding acquisition, X.W. All authors have read and agreed to the published version of the manuscript.

Funding: Natural Science Foundation of China (Grant Nos. U22A2085, 61705091, 61935006, and 62205163); Zhejiang Provincial Natural Science Foundation of China (Grant Nos. LY24F050002, LQ21F050005); Ten-Thousands Talents Program of Zhejiang Province; Leading and top-notch personnel training project of Ningbo; Outstanding talent training program of Jiaying; and the K.C. Wong Magna Fund in Ningbo University.

Institutional Review Board Statement: Not applicable.

Informed Consent Statement: Not applicable.

Conflicts of Interest: The authors declare no conflicts of interest.

References

1. Ke, K.; Xia, C.; Islam, M.N.; Welsh, M.J.; Freeman, M.J. Mid-infrared absorption spectroscopy and differential damage in vitro between lipids and proteins by an all-fiber-integrated supercontinuum laser. *Opt. Express* **2009**, *17*, 12627–12640. [[CrossRef](#)] [[PubMed](#)]
2. Powers, M.A.; Davis, C.C. Spectral LADAR: Active range-resolved three-dimensional imaging spectroscopy. *Appl. Opt.* **2012**, *51*, 1468–1478. [[CrossRef](#)] [[PubMed](#)]
3. Li, C.-H.; Glenday, A.G.; Benedick, A.J.; Chang, G.; Chen, L.-J.; Cramer, C.; Fendel, P.; Furesz, G.; Kärtner, F.X.; Korzennik, S. In-situ determination of astro-comb calibrator lines to better than 10 cm s^{-1} . *Opt. Express* **2010**, *18*, 13239–13249. [[CrossRef](#)] [[PubMed](#)]
4. Yao, C.; Jia, Z.; Li, Z.; Jia, S.; Zhao, Z.; Zhang, L.; Feng, Y.; Qin, G.; Ohishi, Y.; Qin, W. High-power mid-infrared supercontinuum laser source using fluorotellurite fiber. *Optica* **2018**, *5*, 1264–1270. [[CrossRef](#)]
5. Li, Z.; Jia, Z.; Yao, C.; Zhao, Z.; Li, N.; Hu, M.; Ohishi, Y.; Qin, W.; Qin, G. 22.7 W mid-infrared supercontinuum generation in fluorotellurite fibers. *Opt. Lett.* **2020**, *45*, 1882–1885. [[CrossRef](#)] [[PubMed](#)]
6. Zhao, Z.; Wu, B.; Wang, X.; Pan, Z.; Liu, Z.; Zhang, P.; Shen, X.; Nie, Q.; Dai, S.; Wang, R. Mid-infrared supercontinuum covering 2.0–16 μm in a low-loss telluride single-mode fiber. *Laser Photonics Rev.* **2017**, *11*, 1700005. [[CrossRef](#)]
7. Jha, A.; Richards, B.; Jose, G.; Teddy-Fernandez, T.; Joshi, P.; Jiang, X.; Lousteau, J. Rare-earth ion doped TeO_2 and GeO_2 glasses as laser materials. *Prog. Mater. Sci.* **2012**, *57*, 1426–1491. [[CrossRef](#)]
8. Yao, Y.; Yang, F.; Dai, S.; Zhang, P.; Liu, Z.; Qin, G.; Jia, Z. Mid-infrared femtosecond laser-induced damage in TeO_2 - BaF_2 - Y_2O_3 fluorotellurite glass. *Opt. Mater. Express* **2022**, *12*, 1670–1682. [[CrossRef](#)]

9. Takahashi, S. Optical properties of fluoride glasses. *J. Non-Cryst. Solids* **1987**, *95*, 95–106. [[CrossRef](#)]
10. Poulain, M.; Poulain, M.; Lucas, J. Verres fluores au tetrafluorure de zirconium proprietes optiques d'un verre dope au Nd³⁺. *Mater. Res. Bull.* **1975**, *10*, 243–246. [[CrossRef](#)]
11. Whitehurst, C.; Dickinson, M.R.; Charlton, A.; King, T.A.; France, P. Transmission of 2.94 μm laser radiation by zirconium fluoride optical fibers. *Infrared Fiber Opt. Proc. SPIE* **1989**, *1048*, 141–144. [[CrossRef](#)]
12. Wüthrich, S.; Lüthy, W.; Weber, H.P. Optical damage thresholds at 2.94 μm in fluoride glass fibers. *Appl. Opt.* **1992**, *31*, 5833–5837. [[CrossRef](#)] [[PubMed](#)]
13. Nazabal, V.; Poulain, M.; Olivier, M.; Pirasteh, P.; Camy, P.; Doualan, J.L.; Guy, S.; Djouama, T.; Boutarfaia, A.; Adam, J.L. Fluoride and oxyfluoride glasses for optical applications. *J. Fluor. Chem.* **2012**, *134*, 18–23. [[CrossRef](#)]
14. Loehr, S.R.; Bruce, A.J.; Mossadegh, R.; Doremus, R.H.; Moynihan, C.T. IR Spectroscopy Studies of Attack of Liquid Water on ZrF₄-Based Glasses. *Mater. Sci. Forum* **1985**, *5*, 311–322. [[CrossRef](#)]
15. Itoh, K.; Miura, K.; Masuda, I.; Iwakura, M.; Yamashita, T. Low-loss fluorozirco-aluminate glass fiber. *J. Non-Cryst. Solids* **1994**, *167*, 112–116. [[CrossRef](#)]
16. Aydin, Y.O.; Fortin, V.; Vallée, R.; Bernier, M. Towards power scaling of 2.8 μm fiber lasers. *Opt. Lett.* **2018**, *43*, 4542–4545. [[CrossRef](#)] [[PubMed](#)]
17. Slusher, R.; Lenz, G.; Hodelin, J.; Sanghera, J.; Shaw, L.; Aggarwal, I. Large Raman Gain and Nonlinear Phase Shifts in High-Purity As₂Se₃ Chalcogenide Fibers. *J. Opt. Soc. Am. B* **2004**, *21*, 1146–1155. [[CrossRef](#)]
18. Nguyen, V.Q.; Sanghera, J.; Pureza, P.; Kung, F.; Aggarwal, I. Fabrication of Arsenic Selenide Optical Fiber with Low Hydrogen Impurities. *J. Am. Ceram. Soc.* **2002**, *85*, 2849–2851. [[CrossRef](#)]
19. Kapany, N.S.; Simms, R.J. Recent developments in infrared fiber optics. *Infrared Phys.* **1965**, *5*, 69–80. [[CrossRef](#)]
20. Lynda, E.B.; John, A.M.; Jasbinder Singh, S.; Ishwar, D.A. Midinfrared power delivery through chalcogenide glass-clad optical fibers. *Proc. SPIE* **1996**, *2714*, 211–221. [[CrossRef](#)]
21. Sanghera, J.; Shaw, L.; Talley, D.; Busse, L.; Aggarwal, I. IR fiber optics for biomedical applications. *Proc. SPIE—Int. Soc. Opt. Eng.* **2000**, *3907*, 461–467. [[CrossRef](#)]
22. Sanghera, J.S.; Busse, L.E.; Aggarwal, I.D.; Chenard, F. Infrared fibers for defense against MANPAD systems. *Proc. SPIE* **2005**, *5781*, 7–14. [[CrossRef](#)]
23. Papagiakoumou, E.; Papadopoulos, D.N.; Serafetinides, A.A. Pulsed infrared radiation transmission through chalcogenide glass fibers. *Opt. Commun.* **2007**, *276*, 80–86. [[CrossRef](#)]
24. Qi, S.; Li, Y.; Huang, Z.; Ren, H.; Sun, W.; Shi, J.; Wang, F.; Shen, D.; Feng, X.; Yang, Z. Flexible chalcogenide glass large-core multimode fibers for hundred-watt-level mid-infrared 2–5 μm laser transmission. *Opt. Express* **2022**, *30*, 14629–14644. [[CrossRef](#)] [[PubMed](#)]
25. Chenard, F.; Alvarez, O.; Moawad, H. MIR chalcogenide fiber and devices. *Prog. Biomed. Opt. Imaging—Proc. SPIE* **2015**, *9317*, 93170B. [[CrossRef](#)]
26. Sincore, A.; Cook, J.; Tan, F.; El Halawany, A.; Riggins, A.; McDaniel, S.; Cook, G.; Martyshkin, D.V.; Fedorov, V.V.; Mirov, S.B.; et al. High power single-mode delivery of mid-infrared sources through chalcogenide fiber. *Opt. Express* **2018**, *26*, 7313–7323. [[CrossRef](#)] [[PubMed](#)]
27. Liang, X.; Zhong, M.; Xu, T.; Xiao, J.; Jiao, K.; Wang, X.; Yan, B.; Liu, J.; Wang, X.; Zhao, Z. Mid-Infrared single-mode Ge-As-S fiber for high power laser delivery. *J. Light. Technol.* **2022**, *40*, 2151–2156. [[CrossRef](#)]
28. Dianov, E.; Masychev, V.; Plotnichenko, V.; Sysoev, V.; Baikalov, P.; Devjatykh, G.; Konov, A.; Schipachev, J.; Churbanov, M. Fiber-optical cable for CO laser power transmission. *Electron. Lett.* **1984**, *20*, 129–130. [[CrossRef](#)]
29. Hattori, T.; Sato, S.; Fujioka, T.; Takahashi, S.; Kanamori, T. High-power CO laser transmission through As-S glass fibres. *Electron. Lett.* **1984**, *20*, 811–812. [[CrossRef](#)]
30. Arai, T.; Kikuchi, M. Carbon monoxide laser power delivery with an As₂S₃ infrared glass fiber. *Appl. Opt.* **1984**, *23*, 3017–3019. [[CrossRef](#)]
31. Watanabe, S.; Iwamoto, N.; Hattori, T.; Sato, S.-I.; Obara, M.; Takahashi, S.; Kanamori, T. 60-W CO laser power transmission through As-S glass fibers. In Proceedings of the Conference on Lasers and Electro-Optics, Baltimore, ML, USA, 21 May 1985; p. FP6. [[CrossRef](#)]
32. Sato, S.i.; Watanabe, S.; Fujioka, T.; Saito, M.; Sakuragi, S. High power, high intensity CO infrared laser transmission through As₂S₃ glass fibers. *Appl. Phys. Lett.* **1986**, *48*, 960–962. [[CrossRef](#)]
33. Arai, T.; Kikuchi, M.; Saito, M.; Takizawa, M. Power transmission capacity of As-S glass fiber on CO laser delivery. *J. Appl. Phys.* **1988**, *63*, 4359–4364. [[CrossRef](#)]
34. Sato, S.; Igarashi, K.; Taniwaki, M.; Tanimoto, K.; Kikuchi, Y. Multihundred-watt CO laser power delivery through chalcogenide glass fibers. *Appl. Phys. Lett.* **1993**, *62*, 669–671. [[CrossRef](#)]
35. Sanghera, J.S.; Aggarwal, I.D. Active and passive chalcogenide glass optical fibers for IR applications: A review. *J. Non-Cryst. Solids* **1999**, *256–257*, 6–16. [[CrossRef](#)]
36. Nishii, J.; Yamashita, T.; Yamagishi, T. Chalcogenide glass fiber with a core-cladding structure. *Appl. Opt.* **1989**, *28*, 5122–5127. [[CrossRef](#)] [[PubMed](#)]
37. Junji, N.; Ikuo, I.; Syozo, M.; Ryuji, I.; Toshiharu, Y.; Takashi, Y. Chalcogenide glass fibers for power delivery of CO₂ laser. *Proc. SPIE* **1990**, *1228*, 224–232. [[CrossRef](#)]

38. Inagawa, I.; Takashi Yamagishi, T.Y.; Toshiharu Yamashita, T.Y. Transmission-Loss Spectra of Chalcogenide Se-Te-I Glass Fibers and Its Delivery of CO₂ Laser Power. *Jpn. J. Appl. Phys.* **1991**, *30*, 2846. [[CrossRef](#)]
39. Su, J.; Dai, S.; Jiang, L.; Lin, C.; Yang, C.-C.; Zhang, N.; Yuan, Y. Fabrication and bending strength analysis of low-loss Ge₁₅As₂₅Se₄₀Te₂₀ chalcogenide glass fiber: A potential mid-infrared laser transmission medium. *Opt. Mater. Express* **2019**, *9*, 2859–2869. [[CrossRef](#)]
40. Knight, J.; Birks, T.; Russell, P.S.J.; Atkin, D. All-silica single-mode optical fiber with photonic crystal cladding. *Opt. Lett.* **1996**, *21*, 1547–1549. [[CrossRef](#)]
41. Birks, T.A.; Knight, J.C.; Russell, P.S.J. Endlessly single-mode photonic crystal fiber. *Opt. Lett.* **1997**, *22*, 961–963. [[CrossRef](#)]
42. Monro, T.M.; Bennett, P.; Broderick, N.; Richardson, D. Holey fibers with random cladding distributions. *Opt. Lett.* **2000**, *25*, 206–208. [[CrossRef](#)] [[PubMed](#)]
43. Urich, A.; Maier, R.R.J.; Mangan, B.J.; Renshaw, S.; Knight, J.C.; Hand, D.P.; Shephard, J.D. Delivery of high energy Er:YAG pulsed laser light at 2.94 μm through a silica hollow core photonic crystal fiber. *Opt. Express* **2012**, *20*, 6677–6684. [[CrossRef](#)] [[PubMed](#)]
44. Monro, T.M.; West, Y.D.; Hewak, D.; Broderick, N.; Richardson, D.J. Chalcogenide holey fibers. *Electron. Lett.* **2000**, *36*, 1998–2000. [[CrossRef](#)]
45. Troles, J.; Brilland, L.; Smektala, F.; Traynor, N.; Houizot, P.; Desevedavy, F. Chalcogenide Photonic Crystal Fibers for Near and Middle Infrared Applications. In Proceedings of the 2007 9th International Conference on Transparent Optical Networks, Rome, Italy, 1–5 July 2007; pp. 297–300. [[CrossRef](#)]
46. Ren, H.; Qi, S.; Hu, Y.; Han, F.; Shi, J.; Feng, X.; Yang, Z. All-solid mid-infrared chalcogenide photonic crystal fiber with ultralarge mode area. *Opt. Lett.* **2019**, *44*, 5553–5556. [[CrossRef](#)] [[PubMed](#)]
47. Feng, X.; Ren, H.; Xu, F.; Shi, J.; Qi, S.; Hu, Y.; Tang, J.; Han, F.; Shen, D.; Yang, Z. Few-moded ultralarge mode area chalcogenide photonic crystal fiber for mid-infrared high power applications. *Opt. Express* **2020**, *28*, 16658–16672. [[CrossRef](#)]
48. Temelkuran, B.; Hart, S.D.; Benoit, G.; Joannopoulos, J.D.; Fink, Y. Wavelength-scalable hollow optical fibres with large photonic bandgaps for CO₂ laser transmission. *Nature* **2002**, *420*, 650–653. [[CrossRef](#)] [[PubMed](#)]
49. Hayashi, J.G.; Mousavi, S.M.; Ventura, A.; Poletti, F. Numerical modeling of a hybrid hollow-core fiber for enhanced mid-infrared guidance. *Opt. Express* **2021**, *29*, 17042–17052. [[CrossRef](#)]
50. Duguay, M.; Kokubun, Y.; Koch, T.; Pfeiffer, L. Antiresonant reflecting optical waveguides in SiO₂-Si multilayer structures. *Appl. Phys. Lett.* **1986**, *49*, 13–15. [[CrossRef](#)]
51. Benabid, F.; Knight, J.C.; Antonopoulos, G.; Russell, P.S.J. Stimulated Raman scattering in hydrogen-filled hollow-core photonic crystal fiber. *Science* **2002**, *298*, 399–402. [[CrossRef](#)]
52. Pryamikov, A.D.; Biriukov, A.S.; Kosolapov, A.F.; Plotnichenko, V.G.; Semjonov, S.L.; Dianov, E.M. Demonstration of a waveguide regime for a silica hollow—Core microstructured optical fiber with a negative curvature of the core boundary in the spectral region & 3.5 μm. *Opt. Express* **2011**, *19*, 1441–1448. [[CrossRef](#)]
53. Yu, F.; Song, P.; Wu, D.; Birks, T.; Bird, D.; Knight, J. Attenuation limit of silica-based hollow-core fiber at mid-IR wavelengths. *APL Photonics* **2019**, *4*, 080803. [[CrossRef](#)]
54. Gattass, R.R.; Rhonehouse, D.; Gibson, D.; McClain, C.C.; Thapa, R.; Nguyen, V.Q.; Bayya, S.S.; Weiblen, R.J.; Menyuk, C.R.; Shaw, L.B.; et al. Infrared glass-based negative-curvature anti-resonant fibers fabricated through extrusion. *Opt. Express* **2016**, *24*, 25697–25703. [[CrossRef](#)] [[PubMed](#)]
55. Zhang, H.; Chang, Y.; Xu, Y.; Chengzhen, L.; Xiao, X.; li, j.; ma, x.; Wang, Y.; Guo, H. Design and fabrication of a chalcogenide hollow-core anti-resonant fiber for mid-infrared applications. *Opt. Express* **2023**, *31*, 7659–7670. [[CrossRef](#)] [[PubMed](#)]
56. Désévéday, F.; Renversez, G.; Troles, J.; Brilland, L.; Houizot, P.; Coulombier, Q.; Smektala, F.; Traynor, N.; Adam, J.-L. Te-As-Se glass microstructured optical fiber for the middle infrared. *Appl. Opt.* **2009**, *48*, 3860–3865. [[CrossRef](#)] [[PubMed](#)]
57. Kosolapov, A.F.; Pryamikov, A.D.; Biriukov, A.S.; Shiryayev, V.S.; Astapovich, M.S.; Snopatin, G.E.; Plotnichenko, V.G.; Churbanov, M.F.; Dianov, E.M. Demonstration of CO₂-laser power delivery through chalcogenide-glass fiber with negative-curvature hollow core. *Opt. Express* **2011**, *19*, 25723–25728. [[CrossRef](#)]
58. Tong, H.T.; Nishiharaguchi, N.; Suzuki, T.; Ohishi, Y. Mid-infrared transmission by a tellurite hollow core optical fiber. *Opt. Express* **2019**, *27*, 30576–30588. [[CrossRef](#)]
59. Perevoschikov, S.; Kaydanov, N.; Ermatov, T.; Bibikova, O.; Usenov, I.; Sakharova, T.; Bocharnikov, A.; Skibina, J.; Artyushenko, V.; Gorin, D. Light guidance up to 6.5 μm in borosilicate soft glass hollow-core microstructured optical waveguides. *Opt. Express* **2020**, *28*, 27940–27950. [[CrossRef](#)]

Disclaimer/Publisher’s Note: The statements, opinions and data contained in all publications are solely those of the individual author(s) and contributor(s) and not of MDPI and/or the editor(s). MDPI and/or the editor(s) disclaim responsibility for any injury to people or property resulting from any ideas, methods, instructions or products referred to in the content.